Chemistry of Metals and Alloys

Chem. Met. Alloys 1 (2008) 67-72
Ivan Franko National University of Lviv
www.chemetal-journal.org

Phase equilibria in the Ti–$TiMn_2$–$ZrMn_2$–Zr partial system

V.G. IVANCHENKO[1]*, T.V. PRYADKO[1], I.S. GAVRYLENKO[1], V.V. POGORELAYA[1]

[1] *Department of Phase Equilibria, G.V. Kurdyumov Institute for Metal Physics, National Academy of Sciences of Ukraine, Vernadsky Blvd. 36, 03142 Kyiv, Ukraine*
** Corresponding author. E-mail: ivanch@imp.kiev.ua*

Received January 29, 2008; accepted February 17, 2008; available on-line March 31, 2008

The phase equilibria in the Ti–$TiMn_2$–$ZrMn_2$–Zr region of the Ti–Zr–Mn system have been investigated using DTA, X-ray diffraction analysis, optical microscopy and electron microprobe analysis. The solid phases involved are β (Ti,Zr), (Ti,Zr)Mn_2 continuous solid solutions and ρ-TiMn. The liquidus and solidus projections, as well as the $TiMn_2$–$ZrMn_2$, $Ti_{50}Mn_{50}$–$Zr_{50}Mn_{50}$ and $Ti_{60}Mn_{40}$–$Zr_{67.5}Mn_{32.5}$ vertical sections, have been constructed. The phase diagram is characterized by a minimum on the solid surface caused by the existence of a minimum in the Ti–Zr fusibility diagram, and a U-reaction that involves ρ-TiMn, $TiMn_2$ and β-Ti based solid phases and liquid.

Phase equilibria / Phase diagram / Ti-Zr-based alloys / Crystal structure

Introduction

The Ti–Zr–Mn system is of fundamental importance for practical use. Firstly, Zr and Mn are often used as alloying elements in the industry of titanium alloys [1]. Secondly, alloys of this system may be considered as promising candidates for use as hydrogen storage tanks for the proton exchange membrane fuel cell technology [2-4]. Thirdly, the existence of eutectics in the Ti–Mn and Ti–Zr systems with relatively low melting temperatures and the presence of a minimum in the fusibility diagram of the Ti–Zr system design this ternary system as a basic one for developing new solders for reaction brazing of Ti-based alloys and, especially, materials based on titanium aluminide [5]. Knowledge of the constitution of the Ti–Zr–Mn system is therefore important in developing new advanced materials.

Experimental

Alloys were prepared from 99.95 % titanium and 99.95 % zirconium, refined by thermal decomposition of the corresponding iodides, and 99.92 % electrolytic manganese. 30 g ingots were prepared by argon arc melting on a water-cooled copper hearth. After six remeltings, they were casted into a copper mould of 15 mm diameter. The nominal compositions are shown in Table 1. The alloy compositions have been corrected using a FRA 30 spectrometer. The main weight losses were due to Mn evaporation. The Mn relative losses were maximal for alloys with high melting temperatures (Ti-based solid solutions) and reached in this case about 5 % (near 1.5 % in absolute value). The losses for eutectic alloys were negligible. The level of contamination by interstitial elements was less than 0.05 % for oxygen and less than 0.03 % for nitrogen. A portion of each ingot was removed for examination of the cast structure and for DTA in as cast conditions. The remainder was wrapped into titanium foil, placed in an alumina tube, and sealed in a silica tube under partial argon atmosphere. A homogenization anneal of 1 week at 950 ºC was followed by water quenching.

DTA of the as cast alloys and after annealing was performed using the VDTA-8M3 (high-temperature differential thermal analyzer) technique. Y_2O_3 crucibles were used. The rate of heating and cooling was 0.8 ºC/s. The temperatures of phase transformations were measured from the heating curves. The cooling curves were used for qualitative control of the number of phase transformations and to measure the temperature of the beginning of solidification. Solidus temperatures were measured with an accuracy better than ±7 ºC. Fe-K_α, and in some cases Mo-K_α, radiation was used to determine the crystal structures and lattice parameters. X-ray diffraction was carried out on bulk samples, as well as on powder samples. Powder samples were used in the cases where an intermetallic phase was the main phase in the alloy. The lattice parameters were estimated to have an accuracy of ±0.1 %.

Table 1 Nominal compositions of the studied alloys and the DTA results.

No	Composition, at.%			Solidus temperature, °C		Liquidus temperature, °C	Comments on the object of the study
	Ti	Zr	Mn	Experimental	Calculated	Experimental	
1	95	0	5	1540	1534		to give a more precise definition of $\beta/\beta + L$ solidus curve in the Ti–Mn binary system
2	90	0	10	1410	1420		
3	86	0	14	1340	1345		
4	80	0	20	1280	1277		
5	75	0	25	1210	1208		
6	75	2	23	1210	1208		to construct the solidus surface in the titanium corner of the Ti–Zr–Mn phase diagram
7	72	4	24	1175			
8	70	6	24	1072[a]			
9	68	8	24	1065[a]			
10	74	10	16	1200	1195		
11	65	20	15	1050[a]			
12	60	25	15	1055[a]			
13	80	10	10	1340			
14	70	20	10	1208			
15	33.3	0	66.7	1335		1335	to construct the $TiMn_2$–$ZrMn_2$ section
16	25.3	8	66.7	1342		1360	
17	17.3	16	66.7	1375		1410	
18	9.3	24	66.7	1435		1454	
19	2.3	31	66.7	1470		1470	
20	0	33.3	66.7	1450		1450	
21	60	0	40	1175		1175	to construct the $Ti_{60}Mn_{40}$–$Zr_{67.5}Mn_{32.5}$ section along the line connecting the eutectic points in the binary systems
22	58.2	2	39.8	1130		1187	
23	56.44	4	39.56	1100		1190	
24	54.67	6	39.33	1090		1195	
25	50	11.25	38.75	1090		1220	
26	40	22.5	37.5	1058/1090		1240	
27	30	33.75	36.25	1046		1220	
28	20	45	35	1070		1238	
29	10	56.25	33.75	1110/1120		1230	
30	0	67.5	32.5	1125		1125	
31	50	0	50	1225		1275	to construct the $Ti_{50}Mn_{50}$–$Zr_{50}Mn_{50}$ section
32	40	10	50	1175		1313	
33	30	20	50	1075/1090		1369	
34	20	30	50	1040		1424	
35	15	35	50	1048		1428	
36	10	40	50	1063/1075		1428	
37	0	50	50	1130		1420	
38	61	15	24	1085		1160	to give a precise definition of the eutectic line location
39	57	15	28	1087		1090	
40	53	15	32	1087		1127	
41	43	32	25	1040		1068	
42	48	32	20	1040		1042	
43	40	40	20	1070		1075	

[a] Alloy containing the eutectic.

Results and discussion

The Ti–Mn binary system was assessed from [6]. The Mn–Zr system is taken from [7]. The Ti–Zr phase diagram was assessed from [8].

3.1. Polythermal sections, liquidus and solidus projections

The existence of isostructural Laves phases in the Ti–Mn and Mn–Zr systems argues for the formation of continuous solid solutions between $TiMn_2$ and $ZrMn_2$. This assumption was checked by studies of alloys located along the $TiMn_2$–$ZrMn_2$ line, using

DTA and X-ray diffraction. The results of the DTA study are presented in Table 1. It was shown, that this section is pseudobinary. It is characterized by a continuous solid solution between the Laves phases, with a maximum in the fusibility diagram. It is presented in Fig. 1. The composition dependences of lattice parameters show a positive deviation from Vegard's law and may be presented in analytical form for the $(Ti_{1-x}Zr_x)Mn_2$ solid solution as

$a = 0.4833 + 0.0386\ x - 0.019\ x^2 \pm 0.0002$ nm,

$c = 0.7923 + 0.0633\ x - 0.0312\ x^2 \pm 0.0004$ nm.

In graphical form these dependencies are presented in Fig. 2.

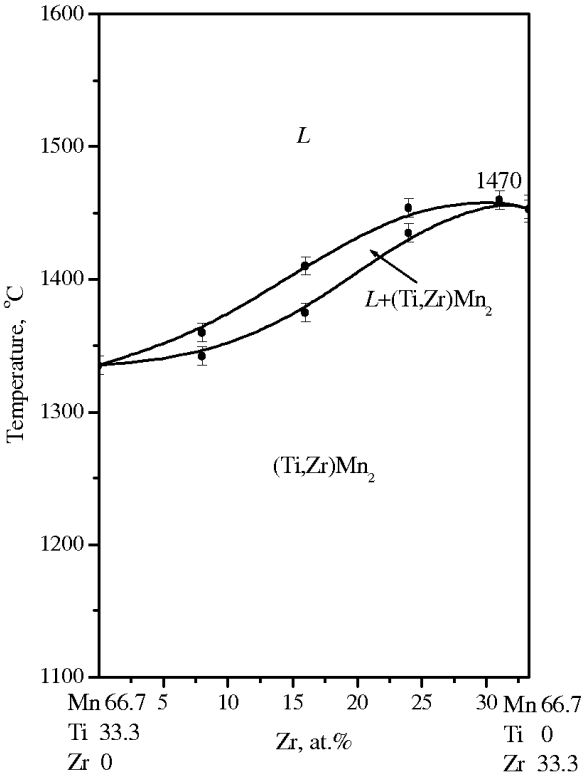

Fig. 1 Quasibinary section $Ti_{33.3}Mn_{66.7}$–$Zr_{33.3}Mn_{66.7}$.

To construct the solidus and liquidus surface projections, alloys located along the $Ti_{50}Mn_{50}$–$Zr_{50}Mn_{50}$ and $Ti_{60}Mn_{40}$–$Zr_{67.5}Mn_{32.5}$ lines were studied. No ternary phases, except the $(Ti_{1-x}Zr_x)Mn_2$ solid solution, were detected. The results obtained by the DTA study of as cast alloys show a smooth transfer from the liquidus with a maximum in the $TiMn_2$–$ZrMn_2$ quasibinary section to the liquidus with a minimum in the Ti–Zr binary system. The solidus surface was smooth and has a minimum at 1040ºC. But one observation might appear somewhat confusing: the study of cast alloys did not show any traces of ρ-TiMn phase formation. Moreover, annealing at 950ºC for 1 week did not lead to the formation of this phase either. Nevertheless, these results were not surprising. During studies of Ti–Mn alloys we faced an analogous problem [9]. The

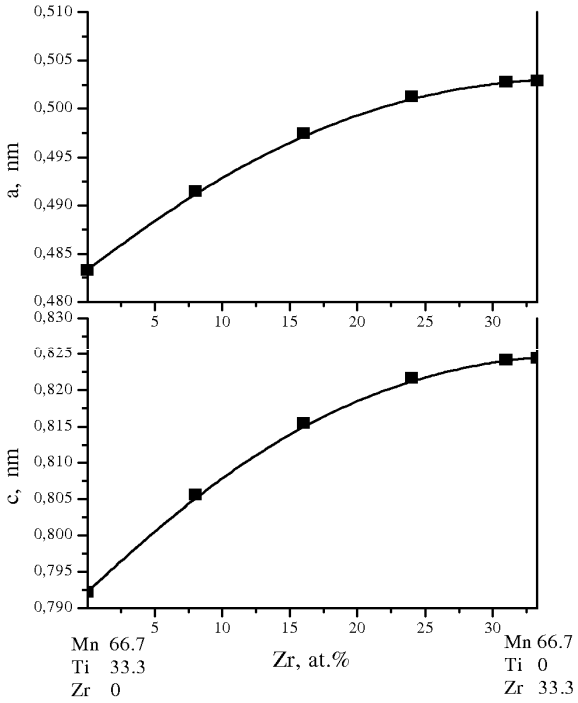

Fig. 2. Composition dependences of the $(Ti_{1-x}Zr_x)Mn_2$ lattice parameters.

diffraction patterns of samples of binary alloys containing 48 and 52 at.% Mn in the as cast and annealed states showed only the presence of $TiMn_2$. These results may be considered as an argument in favor of the absence of the ρ-TiMn peritectic formation. However, a small calorific effect at 1225±10ºC was detected on the heating, as well as on the cooling DTA curves of alloys located in the composition range 48-52 at.% Mn. This effect was absent in the thermogram of $TiMn_2$ (Fig. 3). The weak extra effect in the thermograms reveals a phase transformation at a temperature higher than the melting point of the eutectic. Two samples with 52 and 54 at.% Mn were heated in DTA device to a temperature near the eutectic melting point and annealed in a semi liquid state for 30 min. This heat treatment led to the formation of not only ρ-TiMn, but also ϕ-TiMn. The diffraction patterns were analogous to those obtained after very long annealing by Waterstrat et al. [10]. Analogous experiments were repeated on ternary alloys located close to the TiMn composition (alloys with a Mn content of 48 and 52 at.%, and a Zr content from 2 to 10 at.%). Formation of ρ-TiMn was detected by X-ray diffraction in all these alloys. The compositions of the equilibrium phases taking part in the U-reaction were determined by EPMA. Based on the results obtained by DTA, EPMA and X-ray diffraction the $Ti_{50}Mn_{50}$–$Zr_{50}Mn_{50}$ and $Ti_{60}Mn_{40}$–$Zr_{67.5}Mn_{32.5}$ sections were constructed. They are presented in Fig. 4 and Fig. 5. The projections of the liquidus and solidus surfaces were also constructed and are presented in Figs. 6 and 7.

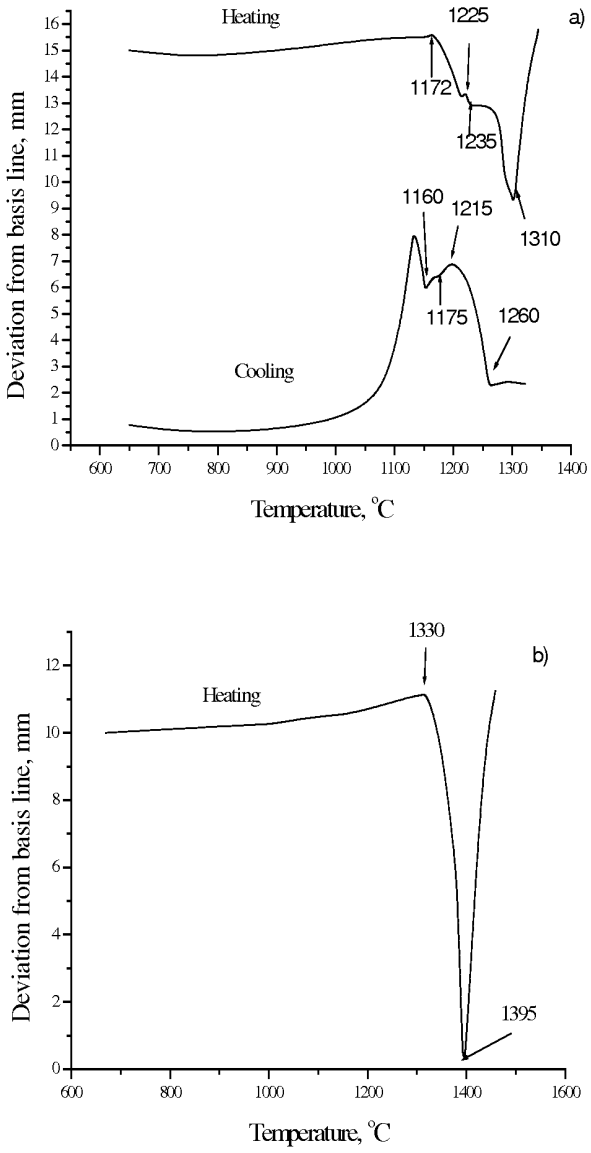

Fig. 3 Heating and cooling curves of $Ti_{50}Mn_{50}$ (a) and heating curve of $Ti_{33}Mn_{67}$ (b) alloys.

The location of the eutectic line was defined more exactly using optical metallography. A typical eutectic structure is presented in Fig. 8. This eutectic may be referred to as a regular type. A fully eutectic structure consists of lamellas or fibers of $(Ti,Zr)Mn_2$ surrounded by transformed β-phase. The solidus surface has a minimum at 1040 °C, located along the $Ti_{70}Zr_{30}$–$Zr_{36}Mn_{64}$ line. This section may be regarded as a quasibinary one, because the eutectic equilibrium is invariant.

The invariant equilibria realized in the composition range studied here are presented in Table 2.

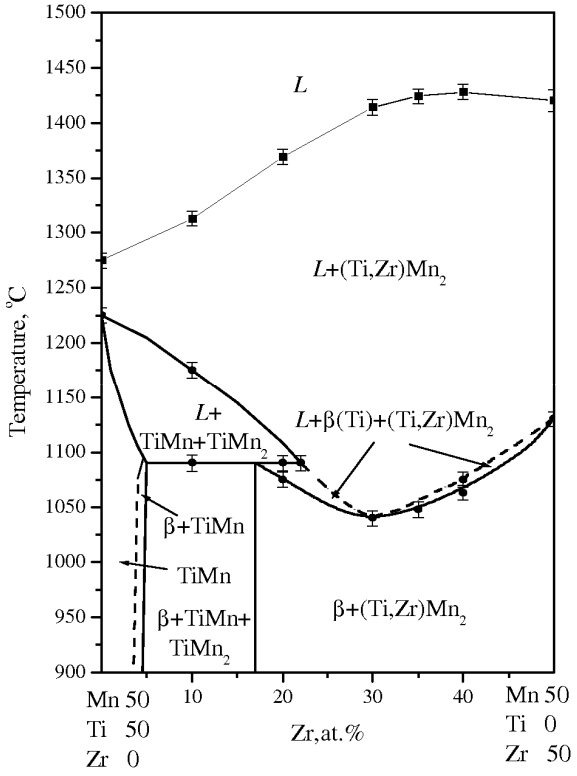

Fig. 4 $Ti_{50}Mn_{50}$–$Zr_{50}Mn_{50}$ section.

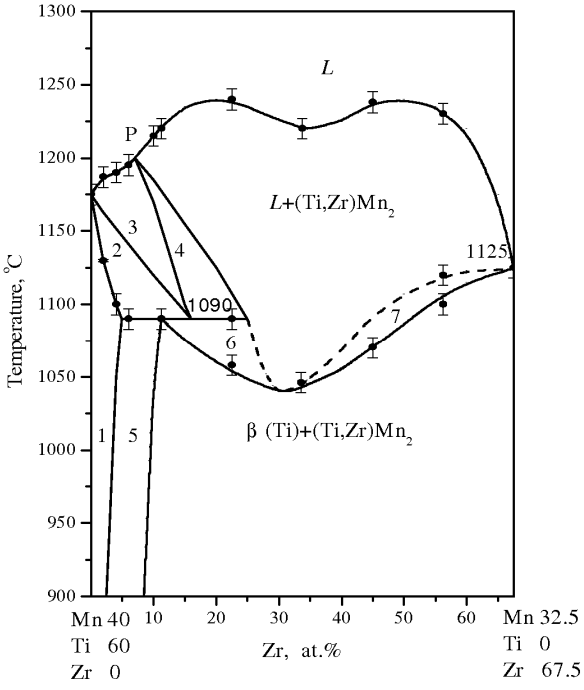

Fig. 5 $Ti_{60}Mn_{40}$–$Zr_{67.5}Mn_{32.5}$ section: (1) β + TiMn; (2) L + β + TiMn; (3) L + TiMn; (4) L + TiMn + $TiMn_2$; (5) β + TiMn + $TiMn_2$; (6), (7) L + β + $TiMn_2$.

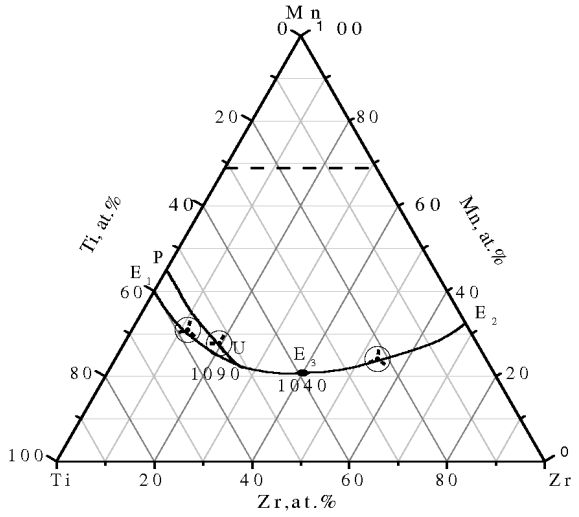

Fig. 6 Liquidus surface of the Ti–$TiMn_2$ – $ZrMn_2$–Zr partial system.

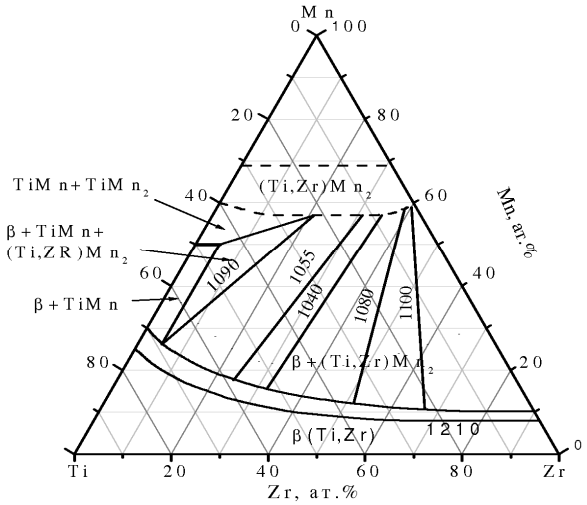

Fig. 7 Solidus surface of the Ti–$TiMn_2$ – $ZrMn_2$–Zr partial system.

Table 2 Invariant equilibria in the Ti–Zr–Mn system

T, ºC Reaction	Type	Phase	Approximate composition, at.%		
			Ti	Zr	Mn
1090		L	51	27	22
L + ρ-TiMn ⇔ β-(Ti) + $(Ti,Zr)Mn_2$	U	ρ-TiMn	45	5	50
		β-(Ti)	69	4	27
		$(Ti,Zr)Mn_2$	23	20	57
1040		L	47	32	21
L ⇔ β-(Ti) + $(Ti,Zr)Mn_2$	E	β-(Ti)	53	32	15
		$(Ti,Zr)Mn_2$	8	35	57
1470		L	2	31	67
L ⇔ $(Ti,Zr)Mn_2$	max.	$(Ti,Zr)Mn_2$	2	31	67

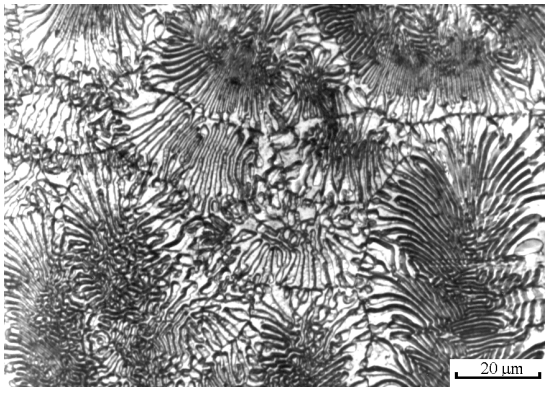

Fig. 8 Microstructure of the eutectic in the 57Ti-15Zr-28Mn alloy.

3.2. Effect of alloying with Mn and Zr on the melting points of Ti-based alloys

As indicated above, the Ti–Zr system is characterized by continuous solid solutions between the high-temperature and low-temperature modifications with a minimum on the fusibility diagram at 35 at.% Zr and 1540 ºC [8]. Alloying of Ti with Mn leads to a decrease of the melting point of β-(Ti) from 1670 ºC to 1181 ºC. At this temperature the eutectic phase equilibrium L (39.2 at.% Mn) ⇔ β-(Ti) (30 at.% Mn) + ρ-TiMn (52 at.% Mn) takes place. Due to the absence of ternary phases in the studied region, the solid surface in the Ti corner of the phase diagram should be smooth and should be described by a power function of the type:

$$T_S = 1670 + \Delta T_S^{Ti\text{-}Zr}(X_{Zr}) + \Delta T_S^{Ti\text{-}Mn}(X_{Mn}) + a\,X_{Zr}\,X_{Mn} + b\,X_{Zr}^2\,X_{Mn} + c\,X_{Zr}\,X_{Mn}^2 \quad (1)$$

where X_{Zr} and X_{Mn} are the concentrations of Zr and Mn (at.%) in the alloys; *a*, *b*, *c* are calculated empirical coefficients; $\Delta T_S^{Ti\text{-}Zr}(X_{Zr})$ and $\Delta T_S^{Ti\text{-}Mn}(X_{Mn})$ are the power parts of the solidus curve equations of the Ti–Zr and Ti–Mn binary systems. To give a more precise definition of the β / β + L solidus curve in the Ti–Mn system, some binary alloys were prepared and studied by DTA. Their compositions, as well as the DTA results, are presented in Table 1. It was found, that the liquidus curve may be presented to high precision by the equation:

$$T_S^{Ti\text{-}Mn} = 1670 - 29.053\,X_{Mn} + 0.4246\,X_{Mn}^2 \quad (2)$$

The results of the experimental measurements are compared with the results of the calculations in

Table 1. The same procedure was repeated for the Ti–Zr system, but with the difference that literature data [8] was used for the calculations. It was found that, in the composition range from zero to 30 at.% Zr, the liquidus curve may be presented as

$$T_S^{Ti\text{-}Zr} = 1670 - 5.692\ X_{Zr} + 0.0566\ X_{Zr}^2 \qquad (3)$$

To calculate the coefficients in equation (1) some ternary alloys were examined. The results are presented in Table 1. The alloys were located along lines with a constant Mn content (24 at.%, 16 at.% and 10 at.%). Some of them (No 8, 9, 11 and 12) included the eutectic. The empirical coefficients of equation (1) were calculated by solving the reverse task after substitution in equation (1) of the power parts of equations (2) and (3) and the solidus temperatures experimentally measured on the alloys No 7, 13 and 14. As a result, the following equation was obtained

$$T_S = 1670 - 29.053\ X_{Mn} + 0.4246\ X_{Mn}^2 - $$
$$- 5.692\ X_{Zr} + 0.0566\ X_{Zr}^2 + 0.6478\ X_{Zr}\ X_{Mn} - $$
$$- 0.0307\ X_{Zr}^2\ X_{Mn} - 0.0065\ X_{Zr}\ X_{Mn}^2. \qquad (4)$$

It was checked on the alloys No 6 and 10. The agreement between the measured and calculated solidus temperatures was excellent (see Table 1). After this, the isotherms at 1540, 1410, 1340, 1280, 1210 and 1175 ºC were calculated. They are presented in Fig. 9. The dashed line is the projection of the line of maximal mutual solubility of Zr and Mn in β-(Ti). It may be noted, that alloying with Zr leads to a strong decrease of the Mn solubility.

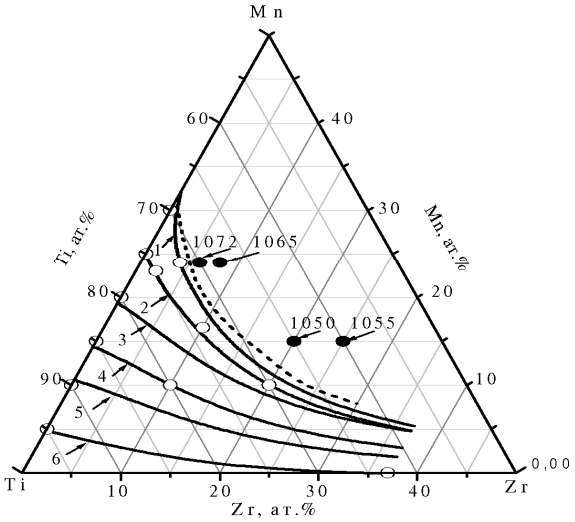

Fig. 9 Solidus surface in the Ti corner of the Mn–Ti–Zr phase diagram.

Conclusions

The $TiMn_2$–$ZrMn_2$ section is quasibinary. It is characterized by continuous solid solutions in the liquid and solid states and the presence of a maximum in the fusibility diagram. Ignoring the $TiMn_2$–$ZrMn_2$ solid solution, ternary phases are absent in the Ti–$TiMn_2$–$ZrMn_2$–Zr composition range.

The $Ti_{50}Mn_{50}$–$Zr_{50}Mn_{50}$ and $Ti_{60}Mn_{40}$–$Zr_{67.5}Mn_{32.5}$ vertical sections have been constructed. They show a smooth transfer from the liquidus with a maximum in the $TiMn_2$–$ZrMn_2$ quasibinary section to the liquidus with a minimum in the Ti–Zr binary system.

The smoothness of the solidus surface is perturbed by the U-reaction ρ-TiMn + L ⇔ β-(Ti) + + $TiMn_2$.

References

[1] S. Lampman, *Metals Handbook*, 10th Ed., Vol. 2, *Properties and Selection: Non Ferrous Alloys and Special Purpose Materials*, ASM International, 1990, p. 592.

[2] S. Semposhi, N. Masahashi, S. Hanada, *J. Alloys Compd.* 352 (2003) 210.

[3] X. Yu, B. Xia, Z. Wu, N. Xu, *Mater. Sci. Eng. A* 537 (2004) 303.

[4] H. Taizong, W. Zhu, Y. Xuebin, Ch. Jinzhou, X. Baojia, X. Tiesheng, X. Naixin, *Intermetallics* 12 (2004) 91.

[5] V.F. Khorunov, S.V. Maksymova, V.G. Ivanchenko, *Adgez. Raspl. Payka Mater.* 37 (2004) 88 (in Russian).

[6] J.L. Murray, *Bull. Alloy Phase Diagr.* 2 (1981) 334.

[7] M.E. Schlesinger, *J. Phase Equilib.* 20 (1999) 79.

[8] J.L. Murray, *Bull. Alloy Phase Diagr.* 2 (1981) 197.

[9] V.G. Ivanchenko, I.S. Gavrylenko, V.I. Nychyporenko, T.V. Pryadko, V.V. Pogorila, *Metaloznav. Obrob. Met.* (4) (2004) 16 (in Ukrainian).

[10] R.M. Waterstrat, B.N. Dass, P.R. Beck, *Trans. AIME* 224 (1962) 512.

Proceeding of the IX International Conference on Crystal Chemistry of Intermetallic Compounds, Lviv, September 20-24, 2005.